SCIENTIFIC REPORTS

OPEN

SUBJECT AREAS:
APPLIED PHYSICS
STATISTICAL PHYSICS
ELECTRONIC AND SPINTRONIC DEVICES
PHOTONIC DEVICES

Received
3 July 2013

Accepted
19 December 2013

Published
27 January 2014

Correspondence and requests for materials should be addressed to R.S.K. (khiminr@gmail.com)

Sensitivity to external signals and synchronization properties of a non-isochronous auto-oscillator with delayed feedback

Vasil S. Tiberkevich[1], Roman S. Khymyn[1,2], Hong X. Tang[3] & Andrei N. Slavin[1]

[1]Department of Physics, Oakland University, Rochester, Michigan 48309, USA, [2]Institute of Magnetism, National Academy of Sciences of Ukraine 03142 Kiev, Ukraine, [3]Department of Electrical Engineering, Yale University, New Haven, Connecticut 06511, USA.

For auto-oscillators of different nature (e.g. active cells in a human heart under the action of a pacemaker, neurons in brain, spin-torque nano-oscillators, micro and nano-mechanical oscillators, or generating Josephson junctions) a critically important property is their ability to synchronize with each other. The synchronization properties of an auto oscillator are directly related to its sensitivity to external signals. Here we demonstrate that a non-isochronous (having generation frequency dependent on the amplitude) auto-oscillator with *delayed feedback* can have an *extremely high sensitivity* to external signals and *unusually large width of the phase-locking band* near the boundary of the stable auto-oscillation regime. This property could be used for the development of synchronized arrays of non-isochronous auto-oscillators in physics and engineering, and, for instance, might bring a better fundamental understanding of ways to control a heart arrythmia in medicine.

The systems with auto-oscillation properties are common in science and nature starting from a simple pendulum clock and ending with complex neural systems of animals and humans. In general, every auto-oscillator consists of an active element (source of energy) and a passive oscillating system, which converts the energy obtained from the active element to the energy of oscillations and determines the oscillation frequency. In electronics auto-oscillators are used for the generation of periodic signals and in digital systems as clocks that synchronize the system operation. Similarly, mechanical oscillators, such as quartz oscillators, play a dominant role in today's time keeping devices[1]. Auto-oscillating systems are also well known in biology[2], chemistry[3], and even economics[4].

In applications, one of the most important characteristics of an auto-oscillator is its generation linewidth which is determined by the auto-oscillator interaction with noise[1]. On the other hand, an equally important characteristic of an auto-oscillator is its ability to synchronize with other auto-oscillators. This property is important for the understanding of the behavior of coupled ensembles of auto-oscillators. In a broader sense, synchronization is a property of an ensemble of auto-oscillators that allows it to behave as a single entity[5]. In particular, synchronization properties are very important in biological systems, where each cell of a tissue acts as a single auto-oscillator, while the population of these cells (e.g. the entire organism, or even a group of organisms) acts as a single auto-oscillating system consisting of an array of coupled and synchronized auto-oscillators. There are, also, many examples of auto-oscillator arrays in physics and microwave electronics (see e.g. generating Josephson junctions[6] or spin-torque nano-oscillators (STNO)[7–10]) for which synchronization properties are extremely important, because individual auto-oscillators have a relatively low output power and the action of a synchronized array is necessary for practical applications of these devices.

It should be noted, that the generation linewidth of an auto-oscillator, as well as its phase-locking bandwidth to an external periodic signal and its synchronization bandwidth with other auto-oscillators, are determined by the same property of an auto-oscillating system – its sensitivity to an external signal, be it an external noise or a periodic driving signal generated by an external driver or by other auto-oscillators in the ensemble.

To determine this sensitivity we need, at first, to qualitatively understand how a typical auto-oscillator reacts on the amplitude and phase fluctuations. In a steady-state auto-oscillation a flow of energy from an active element,

producing a nonlinear negative damping, is compensated by the absorption of this flow by a dissipative element, providing a positive damping, which, in a general case, can also be nonlinear[7]. Thus, the condition of a zero total damping or, in other words, the condition of a dynamic equilibrium between the energy taken from an active element and absorbed by a dissipative element of an auto-oscillator, defines the stable limit cycle of an auto-oscillation. In such a situation, the fluctuations of the auto-oscillation amplitude (or of the effective radius of the limit cycle) introduced into the system may shift the system trajectory from the limit cycle, but the above mentioned dynamic equilibrium condition will return the system back to the limit cycle after a finite time. The situation is drastically different with the phase fluctuations (or shifts *along* the limit cycle). Since the system has no mechanism to return to the initial phase, the phase fluctuations perform a random walk and accumulate over time. Thus, the auto-oscillating systems are particularly sensitive to the *phase* fluctuations, and the experimentally observed generation linewidth of a typical auto-oscillator is, for the most part, determined by the phase fluctuations[11–17]. Analogously, when the external signal is periodic (e.g. when it is created by an external driver or by another auto-oscillator) the phase sensitivity mostly determines the *phase-locking bandwidth* of an auto-oscillator – the maximum deviation of the frequency of an external driving signal from the generation frequency of the auto-oscillator at which the auto-oscillation phase still follows the phase of the external signal[5,18–21].

As it was explained above, the stable limit cycle and, therefore, the steady-state amplitude in an auto-oscillating system is determined by the nonlinearity of its negative and positive damping. At the same time, the equilibrium auto-oscillation frequency is determined by the passive oscillating system, which can also be nonlinear, resulting in the non-isochronous property of the auto-oscillator – dependence of the auto-oscillation frequency on the auto-oscillation amplitude. Besides, in many cases the process of the energy transfer from an active element to a passive oscillating system may take much more time then one period of oscillation. In such a situation, typical for the systems with spatially distributed parameters, the dynamics of an auto-oscillating system can be strongly influenced by the time delay existing in it.

It turns out, that many of the practically interesting auto-oscillating systems are both *non-isochronous* and have a *delayed feedback*. One such example is an optoelectronic oscillator based on a low-loss delay line[1]. Another example of such an auto-oscillating system is a heart of a mammal. In a bloodstream of a mammal the arterial pressure plays a role of a signal, while the arterial baroreceptors, vasculature, and central nervous system process this signal in the feedback lines with significant delays[22]. Also, the frequency of the heartbeat is changing with the heartbeat amplitude, so this auto-oscillating system is also non-isochronous.

A concept of a non-isochronous auto-oscillator with delay is also widely used to describe the activity of neurons in the brain of animals. In the neurons inside the brain the large time delays in the feedback are caused by the signal processing in the whole neural network[2,23,24].

In biology, one of the most explicit examples of a non-isochronous auto-oscillating system with delayed feedback is the locomotion of fish and reptiles[25,26]. The generator in the central nervous system (CNS) of a fish produces periodic oscillations that move through the spinal cord to muscles and resemble waves propagating in a transmission line. Specific receptors capture these waves and send a feedback signal to the CNS.

In all the above presented examples it is very important to understand the detailed behavior of the sensitivity of a non-isochronous auto-oscillating system with delay to an external signal, as the abnormal values of this sensitivity could cause serious irregularities in the system function, which in biological systems manifest themselves as diseases. For example, the abnormal increase of the phase sensitivity of a human heart causes arrythmia, while its abnormal decrease leads to serious medical conditions after the heart transplantation.

In the framework of a general theory of dynamical systems an auto-oscillator driven by an external force is described by the equation:

$$d\boldsymbol{x}(t)/dt = \boldsymbol{f}[\boldsymbol{x}(t)] + \boldsymbol{\xi}(t), \tag{1}$$

where $\boldsymbol{x}(t)$ is the vector describing the state of an auto-oscillator, function $\boldsymbol{f}[\boldsymbol{x}(t)]$ defines all the internal properties of an auto-oscillator, and $\boldsymbol{\xi}(t)$ is a weak external driving signal. This equation can be reduced to the so-called phase model:

$$d\phi(t)/dt = \omega_0 + \boldsymbol{X}[\phi(t)]\cdot\boldsymbol{\xi}(t), \tag{2}$$

where $\phi(t)$ and ω_0 are, respectively, the auto-oscillation phase and frequency, while $\boldsymbol{X}[\phi(t)]$ is the so-called *sensitivity function* or phase response function, that describes the reaction of the auto-oscillator's phase on the external perturbation[27,28].

Unfortunately, this elegant scheme cannot be used directly to describe auto-oscillators with delayed feedback. Indeed, even in a simplest case of an oscillator with delayed feedback the function $\boldsymbol{f}$ in Eq. (1) becomes dependent on the delayed oscillator's state $\boldsymbol{x}(t-T)$ (T is the delay time), $\boldsymbol{f} = \boldsymbol{f}[\boldsymbol{x}(t), \boldsymbol{x}(t-T)]$. Thus, the equation for an oscillator with delay can be written in the form of Eq. (1) only by introducing an *infinite-dimensional* state vector $\tilde{\boldsymbol{x}}(t) = [\boldsymbol{x}(t), \boldsymbol{x}(t-T), \boldsymbol{x}(t-2T)\ldots]$ and an external force $\tilde{\boldsymbol{\xi}}(t) = [\boldsymbol{\xi}(t), \boldsymbol{\xi}(t-T), \boldsymbol{x}(t-2T)\ldots]$. Respectively, the vector sensitivity function $\boldsymbol{X}(\phi)$ also becomes infinitely-dimensional, which makes phase model Eq. (2) unsuitable for practical calculations.

This difficulty is the main reason why, despite a number of interesting results obtained in the theory of coupled oscillators with delay in the inter-oscillator coupling[29–32], in the majority of existing theoretical papers describing the dynamics of auto-oscillating systems (see e.g.[11–13]) the time delay in the feedback loop of an auto-oscillator itself is either ignored or is considered as a small correction[31].

In our current paper we found an auto-oscillator model which allows one to formally take into account the time delay in an auto-oscillator feedback loop. In the framework of this model an auto-oscillator consists of two parts: a *linear* resonant part, which defines the auto-oscillating frequency and contains linear elements providing delay in feedback, and a *nonlinear* part containing an active element that provides negative damping and is responsible for the auto-oscillator's non-isochronous properties. Using this model it is possible to analytically calculate the *sensitivity* $X[\phi(t)]$ to an external signal of a *non-isochronous auto-oscillator with delayed feedback* and to evaluate all the non-autonomous properties of such an auto-oscillator determined by this sensitivity. Although our model is less general than the model (1), it, nonetheless, describes most of non-isochronous auto-oscillators with delayed feedback that are practically important in physics, biology and electronics.

Results

A model of a non-isochronous auto-oscillator with delayed feedback. The non-autonomous behavior of a wide range of auto-oscillators can be described by a simple model of a closed auto-oscillating loop (see Fig. 1) that consists of a nonlinear amplifier (active element), a linear resonance oscillating system (which may contain an element causing the signal delay, e.g. a delay line), and a source of a relatively weak (compared to the auto-oscillation amplitude) external signal, which may be either stochastic (noise) or/and periodic (driving signal).

The nonlinear active element, described by the function $G(p)$, where p is the oscillation power, provides the energy flow into the system, while the passive linear oscillating system, described by the linear operator L ($i\,d/dt$), determines the auto-oscillation frequency and provides positive damping, or energy sink. In this approach, the active element is assumed to have an infinite frequency bandwidth, so the output signal of the active element depends only on the

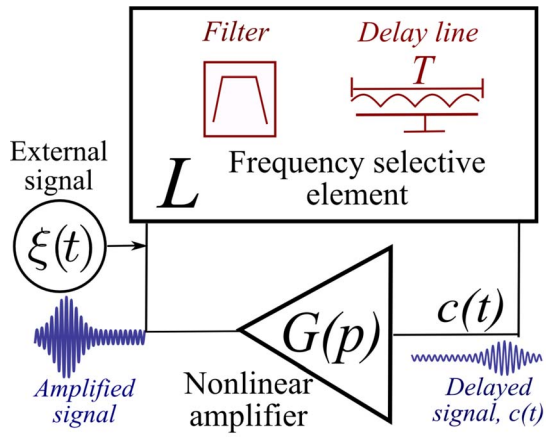

Figure 1 | Schematic view of the oscillator described by equation (3).

instantaneous value of the input signal. The corresponding operator equation written in the time domain and describing such a system has the form:

$$L^{-1}(i\,d/dt)c(t) - G(p)c(t) = \xi(t), \tag{3}$$

where the function $c(t)$ describes the complex amplitude of the auto-oscillation at the input of the nonlinear active element, $p = |c(t)|^2$ is the signal power, and the function $\xi(t)$ describes a weak external driving signal acting on the auto-oscillating loop. Please, note that the dimension of the external signal $\xi(t)$ differs from the dimension of $c(t)$ by the dimension of the linear operator L.

In the frequency domain the operator $L\,(i\,d/dt)$ can be described by a transfer function $L(\omega)$ that is defined as a Fourier transform of the impulse response function of the oscillating system and can be directly measured experimentally.

We stress, that in the model equation (3) the operator $L\,(i\,d/dt)$ describing the oscillating system with delay is *linear*, so that the non-isochronous properties of the auto-oscillator (i.e., the dependence of the oscillation frequency ω on the oscillation power p), as well as the nonlinear properties of the active element limiting the auto-oscillation amplitude and defining the limit cycle, are described by the nonlinear amplifier gain $G(p)$.

The model (3) describes, either directly or after an appropriate change of variables, a vast variety of natural and artificial auto-oscillating systems. A few particular examples will be given below (see section "Examples").

In the absence of external perturbations ($\xi(t) = 0$) we assume the stationary auto-oscillations at a limit cycle of the auto-oscillator Fig. 1 to be harmonic, and the stationary solution for the function $c(t)$ has the form:

$$c_s(t) = \sqrt{p_s}e^{-i\phi(t)}, \tag{4}$$

where $\phi(t) = \omega_s t + \phi_0$, p_s and ω_s are the stationary free-running auto-oscillation power and frequency, respectively, and ϕ_0 is an arbitrary initial phase of the auto-oscillation. The parameters p_s and ω_s of the stationary auto-oscillation are determined by the following amplitude and phase conditions, which directly follow from equation (3):

$$\begin{aligned} &\mathrm{abs}[L\,(\omega_s)\;G\,(p_s)] = 1, \\ &\arg[\,L(\omega_s)] + \arg[G\,(p_s)] = 2\pi n, \end{aligned} \tag{5}$$

where $n = 1, 2, 3, \ldots$ is an integer number.

In a general case the conditions(5) for stationary auto-oscillations define many different auto-oscillation modes which reflects the multi-mode nature of the auto-oscillator loop Fig. 1 (see the mode spectrum shown in Fig. 2). Which one of the possible auto-oscillation modes will be actually generated in the auto-oscillator is determined by the relative stability properties of the stationary solutions of equation (5), which can be analyzed using the central equation of our model (3).

Sensitivity of an auto-oscillator to external perturbations. In the presence of a *weak* external signal $\xi(t)$, both the frequency and the power of the auto-oscillation will experience slight shifts from their stationary values, and the non-autonomous properties of the perturbed auto-oscillator will depend on the behaviour of the functions $L(\omega)$ and $G(p)$ in the vicinity of the limit cycle, which corresponds to the stable auto-oscillation mode (p_s, ω_s). The parameters determining the non-autonomous dynamics of the auto-oscillator can be obtained by expanding the functions $L(\omega)$ and $G(p)$ in a Taylor series near the limit cycle (p_s, ω_s):

$$\begin{aligned} T &= -i\left.\frac{\partial L(\omega)/\partial\omega}{L(\omega_s)}\right|_{\omega=\omega_s}, \\ \beta &= -p_s\left.\frac{\partial G(p)/\partial p}{G(p_s)}\right|_{p=p_s}. \end{aligned} \tag{6}$$

Both parameters T and β are, in general, complex quantities that have a simple physical meaning. The real part of T ($\mathrm{Re}(T)$) acts as an effective delay time in the feedback loop. The imaginary part of T ($\mathrm{Im}(T)$) characterizes the slope of the transfer function $L(\omega)$ at the frequency ω_s of the stationary auto-oscillation (see Fig. 2). The real part of β ($\mathrm{Re}(\beta) = \beta_r$) – *amplifier nonlinearity*, characterizes the dependence of the gain of the active element on the oscillation power. In most cases β_r is positive ($\beta_r > 0$) which means that the amplifier gain decreases with power and this effect limits the auto-oscillation amplitude. The imaginary part of β ($\mathrm{Im}(\beta) = \beta_i$) – *nonlinear frequency shift*, determines the dependence of the auto-oscillation frequency on power, and, therefore, describes the non-isochronous properties of the auto-oscillator.

Under the influence of an external time-dependent signal the phase ϕ_0 in equation (4) becomes a function of time. Assuming that the external signal $\xi(t)$ is weak and, therefore, can only slowly change the phase and slightly vary the amplitude of the auto-oscillation, we derived the following approximate equation describing the phase dynamics of the auto-oscillation in time:

$$\frac{d\phi(t)}{dt} = \omega_s - \mathrm{Im}\left[\chi\xi(t)e^{i\phi(t)}\right], \tag{7}$$

where χ can be defined as phase sensitivity of a non-isochronous auto-oscillator to an arbitrary external signal $\xi(t)$. Such a result for the phase model of equation (2) was, of course, expected due to the simple form of equation (4), which means the circular shape of the limit cycle on the phase plane.

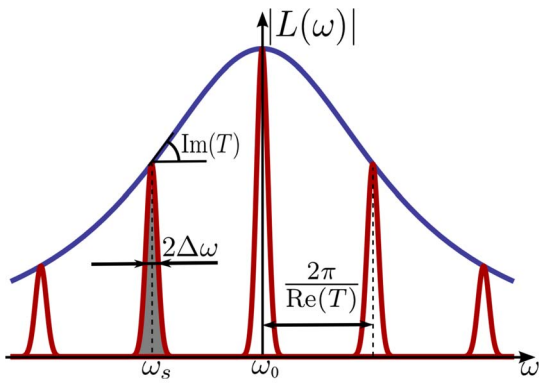

Figure 2 | Transfer function (blue) and mode spectrum (red) of the auto-oscillator. Generation line is shown by filling under the curve.

In the framework of the approximate phase equation (7) the finding of all the non-autonomous characteristics of an auto-oscillator, such as the generation linewidth, phase-locking bandwidth to the external periodic signal, or the synchronization frequency band with other similar auto-oscillators, can be reduced to finding the auto-oscillator sensitivity χ. The solution of equation (3) near the auto-oscillation limit cycle (see "Methods") leads to the following expression for the auto-oscillator sensitivity χ:

$$\chi = \frac{L(\omega_s)\beta}{\sqrt{p_s}\mathrm{Re}(\beta^* T)}, \tag{8}$$

where β* is the complex conjugate of β.

When the auto-oscillator sensitivity χ is known, it is easy, using equation (7) and equation (8), to evaluate the frequency phase-locking bandwidth of an auto-oscillator to an external periodic signal of the amplitude A:

$$\Delta\omega_{PL} = A|\chi| = \frac{A|\beta||L(\omega_s)|}{\sqrt{p_s}\mathrm{Re}(\beta^* T)}. \tag{9}$$

Similarly, using equation (7) and equation (8), it is easy to evaluate the generation linewidth of an auto-oscillator. In the presence of thermal noise the auto-oscillator phase ϕ performs a random walk with the phase variance linearly increasing with time and the generation line of the auto-oscillator has a Lorentzian shape with the linewidth $2\Delta\omega$ (full width at half maximum (FWHM)) evaluated as:

$$2\Delta\omega = \frac{1}{2}|\chi|^2 \mathcal{S}_n(\omega_s) = \frac{|\beta|^2 |L(\omega_s)|^2 \mathcal{S}_n(\omega_s)}{2p_s[\mathrm{Re}(\beta^* T)]^2}, \tag{10}$$

where $\mathcal{S}_n(\omega_s)$ is the spectral density of the noise power calculated at the frequency of the stationary auto-oscillation. The spectrum of the thermal Johnson-Nyquist noise could be written as (see equation (92) in[7])

$$\mathcal{S}_n(\omega) = 2\Gamma p_n, \tag{11}$$

where p_n is the noise power (power of the oscillations in the system in the thermal equilibrium state) and Γ is the damping parameter of the loop.

One interesting and non-trivial consequence of the general expression (8) is the fact that the auto-oscillator sensitivity χ, and, therefore, the phase-locking bandwidth and the generation linewidth, diverge when Re (β*T) = 0. Thus, near this point the auto-oscillator is very sensitive to the external signal and will easily phase lock to an external driver or easily synchronize with other similar auto-oscillators. Therefore, the study of the auto-oscillator behavior in the vicinity of the point where Re (β*T) = 0 is very important for practical applications, and, if such regimes of stable auto-oscillations exist, they can be used for the synchronization of arrays of auto-oscillators, even in the case when their auto-oscillation frequencies are not very close to one another.

Below, we present several examples of application of the general expression (8) to different auto-oscillating systems.

Applications to simple auto-oscillating systems. *Isochronous (β_i = 0) auto-oscillator generating at resonance (ω_s = ω_0).* The model equation (3) covers a wide range of auto-oscillators of different physical nature, and it can be shown that in simple particular cases the expression for the generation linewidth (10) following from this model can be reduced to well-known results.

For the isochronous auto-oscillator where the oscillation system is a simple LCR circuit with a quality factor $Q = \omega_s/2\Gamma$, where Γ is a damping parameter, the transfer function can be represented in a simple Lorentzian form

$$L(\omega) = \frac{1}{\Gamma - i(\omega - \omega_0)}. \tag{12}$$

In this case the generation frequency coincides with the resonance frequency of the oscillating system (LCR circuit), $\omega_s = \omega_0$. Thus, the effective delay time is real and is given by $T = 1/\Gamma = 2Q/\omega_s$. If the phase shift of oscillations at the amplifier output does not depend on power, the nonlinearity β contains only the real part, $\beta = \beta_r$, and the function $G(p)$ in the vicinity of the stationary point can be written as:

$$G(p) = K[1 - \beta_r(p - p_s)/p_s], \tag{13}$$

where the amplifier gain K should be chosen to satisfy the amplitude condition of the stationary generation (the first condition in equation (5)), which leads to $K = \Gamma$. Thus, the general expression for the auto-oscillator generation linewidth (10) is reduced to a well-known result[7,11]:

$$2\Delta\omega_0 = \frac{\omega_s}{2Q}\frac{p_n}{p_s} = \Gamma\frac{p_n}{p_s} \tag{14}$$

Non-isochronous ($\beta_i \neq 0$) auto-oscillator generating at resonance (ω_s = ω_0). In a non-isochronous auto-oscillator the nonlinearity parameter has both real and imaginary parts, $\beta = \beta_r + i\beta_i$, and the imaginary part β_i describes the non-isochronous properties of the auto-oscillator. The typical example of such an auto-oscillator is a spin-torque nano-oscillator (STNO) which can be described by the equation[7]:

$$\frac{dc(t)}{dt} + i\omega(p)c(t) + \Gamma_{tot}(p)c(t) = \xi(t), \tag{15}$$

where Γ_{tot} contains both the natural positive linear damping Γ and the positive and negative nonlinear damping $\Gamma_{nl}(p)$. Separating linear and nonlinear parts in both $\Gamma_{tot}(p)$ and $\omega(p)$ one gets:

$$\begin{aligned} \Gamma_{tot}(p) &= \Gamma + \Gamma_{nl}(p), \\ \omega(p) &= \omega_0 + \omega_{nl}(p). \end{aligned} \tag{16}$$

Then, the linear transfer function $L(\omega)$ can be represented in the Lorentzian form (12) and the "amplifier" nonlinear function has the form:

$$G(p) = -\Gamma_{nl}(p) - i\omega_{nl}(p). \tag{17}$$

Calculating the values for β and T from the above equations, one can get the auto-oscillator generation linewidth from equation (10) in the form[7]:

$$2\Delta\omega = (1 + v^2)\Gamma\frac{p_n}{p_s} = 2\Delta\omega_0(1 + v^2), \tag{18}$$

where $v = \beta_i/\beta_r = (d\omega/dp)/(d\Gamma_{tot}/dp)$.

Non-isochronous ($\beta_i \neq 0$) auto-oscillator generating off resonance ($\omega_s \neq \omega_0$). The qualitatively new results are obtained from equations (8–10) when both parameters T and β are complex. A sample equation describing an auto-oscillator with complex T and β can be written in the form:

$$\begin{aligned} &\frac{dc(t)}{dt} + [i\omega_0 + \Gamma]c(t) - K\left[1 - \beta_r\frac{|c(t-\tau)|^2 - p_s}{p_s}\right] \times \\ &\times \exp\left[-i\beta_i\frac{|c(t-\tau)|^2 - p_s}{p_s}\right]c(t-\tau) = \xi(t). \end{aligned} \tag{19}$$

In the auto-oscillating system described by equation (19) the linear transfer function $L(\omega)$, compared to equation (12), has an additional multiplier which explicitly contains the delay time τ and should be written as

$$L(\omega) = \frac{\exp(i\tau\omega)}{\Gamma - i(\omega - \omega_0)}, \tag{20}$$

while the nonlinear amplifier function $G(p)$ also contains an additional multiplier responsible for nonlinear frequency shift and has the form:

$$G(p)=K\left(1-\beta_r\frac{p-p_s}{p_s}\right)\exp\left(-i\beta_i\frac{p-p_s}{p_s}\right). \qquad (21)$$

Using the above presented expressions for $L(\omega)$ and $G(p)$ it is easy to calculate the auto-oscillator parameters equation (6) at the stationary frequency $\omega_s \neq \omega_0$:

$$\begin{aligned}\beta&=\beta_r+i\beta_i,\\ T&=\tau+1/(\Gamma+i\delta\omega_0),\end{aligned} \qquad (22)$$

where $\delta\omega_0 = \omega_0 - \omega_s$. The amplifier gain K is chosen to provide the stationary generation at the frequency $\omega = \omega_s$ satisfying conditions equation (5). The equation (19) is also convenient for the numerical analysis of the problem.

The condition $\mathrm{Re}(\beta^*T) = 0$ for the singularity in the expression (8) for the phase sensitivity of an auto-oscillator can be rewritten as an equation of a straight line on the plane (β_r, β_i):

$$\beta_i=\frac{\beta_r}{\delta\omega_0}\left[\Gamma+\left(\delta\omega_0^2+\Gamma^2\right)\tau\right]. \qquad (23)$$

The condition $\mathrm{Re}(\beta^*T) = 0$ (see the solid red line in Fig. 3a) also defines the boundary of the auto-oscillation stability region in respect to low-frequency modulation of the generated signal. The other boundaries of the stability region (shown by black solid lines in Fig. 3a) are the boundaries of the stability region in respect to the decay into different auto-oscillation modes (see Fig. 2). These boundaries are found from the numerical solution of equation (19).

We would like to note, that normally the negative sign of the amplifier nonlinearity $\beta_r < 0$, corresponding to the case when the amplification gain *increases* with the increase of the oscillation power p, automatically leads to the instability of the auto-oscillation regime. However, if $\beta_i \neq 0$, the stable auto-oscillations can exist even if the product $\beta_i\beta_r$ is negative. On the other hand, when the real part of the auto-oscillator nonlinearity is positive $\beta_r > 0$ the region of stability of the auto-oscillations is much wider, and the stable auto-oscillations are possible for any sign of the product $\beta_i\beta_r$.

The phase-locking bandwidth of the auto-oscillator to an external signal (relative to the linear damping Γ of the oscillating system) is shown in Fig. 4 in a logarithmic scale. It is clearly seen from Fig. 4 that as soon as the system gets close to the low-frequency boundary (23) of the stability region (shown by the solid red line in Fig. 3), the phase-locking bandwidth drastically increases. The similar behavior is demonstrated by the graph of the auto-oscillator generation linewidth (see Fig. 5). The numerical calculations confirm that the oscillations remain stable when the system approaches the boundary of the stability region.

Two coupled auto-oscillators. To illustrate the qualitative influence of the increase in auto-oscillator sensitivity near the line $\mathrm{Re}(\beta^*T) = 0$ on the behavior of coupled auto-oscillator arrays we considered an elementary example of a coupled pair of practically identical auto-oscillators that have slightly different generation frequencies, separated by the interval $\delta\omega_0 = \omega_0 - \omega_s$, and different initial phases. Both auto-oscillators in a coupled pair are described by the same model(19), where the external signal in the right-hand-side part $\xi_{1,2}(t) = a_{1,2}c_{2,1}(t)$ is proportional (with a coupling constant $a_{1,2}$) to the oscillation amplitude of the other oscillator.

We numerically calculated the phase difference $\Delta\phi$ between the oscillations of the two coupled oscillators in two different cases (see Fig. 3a): when the parameters of the coupled auto-oscillators were close to the low-frequency boundary of the auto-oscillation stability region (left blue point in Fig. 3a) and when auto-oscillators parameters were far from that boundary (right red point in Fig. 3a). The evolution of the phase difference in the pair of coupled oscillators with time in these two cases are shown in Figs. 3b and c, respectively, where different colors correspond to different initial phase differences between the oscillators. As one can see, in the first case (Fig. 3b)

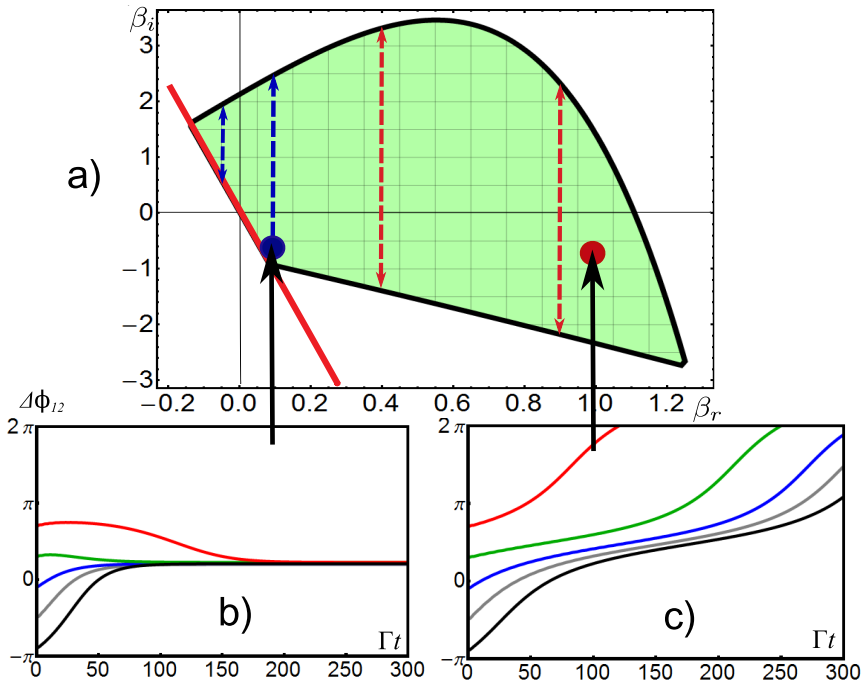

Figure 3 | (a) Stability diagram for $\tau = 3/\Gamma$, $\delta\omega_0 = \omega_0 - \omega_s = 0.4\Gamma$. Region of the stable generation is shown by green color. Arrows correspond to the calculated plots in Figs. 4 and 5. (b) and (c) Time evolution of the phase difference between two coupled auto-oscillators with parameters close (b) $\beta_r = 0.07$ and far (c) $\beta_r = 1$ from the low-frequency boundary of the auto-oscillation stability region. Different colours correspond to different *initial* phase differences between the coupled auto-oscillators. Other parameters (common for both oscillators) used in calculations: $\beta_i = -0.7$, $\delta\omega_{0,1} = 0.4\Gamma$, $\delta\omega_{0,2} = 0.37\Gamma$, $a_1 = a_2 = 0.04\Gamma$.

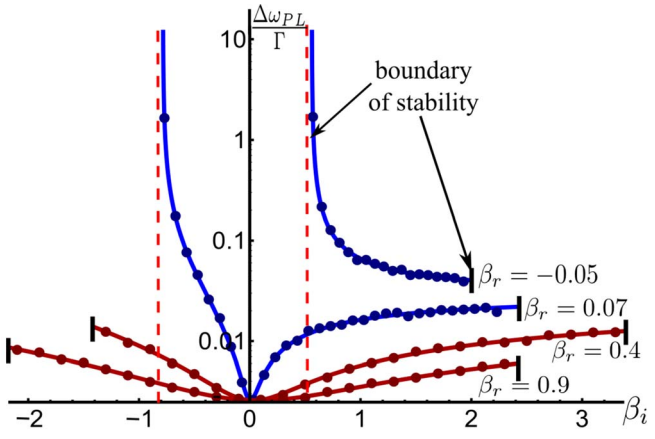

Figure 4 | Dependence of the phase-locking bandwidth on the factor of nonlinear frequency shift β_i in the stability region for different values of the amplifier nonlinearity β_r for $A/(\Gamma\sqrt{ps}) = 0.01$. Analytical results of the equation (9) are shown by solid lines, numerical results obtained from equation (19) are shown by dots. Color of the plots corresponds to the color of the arrows in Fig. 3.

of large sensitivity any initial phase difference $\Delta\phi$ between the coupled oscillators is rapidly reduced to zero demonstrating effective synchronization, while in the second case of relatively low sensitivity the initial phase difference grows with time and no synchronization is observed.

It should be noted, that in this particular case the presence of the delay time in the feedback loop, in contrast to the case of synchronization of two auto-oscillators with a delayed coupling[29], does not lead to the existence of several synchronization frequencies and corresponding phase shifts. However, in principle, the delay time in the feedback loop defines the eigenfrequencies of the auto-oscillator by the equation (5), and can lead to a multi-mode auto-oscillation regime.

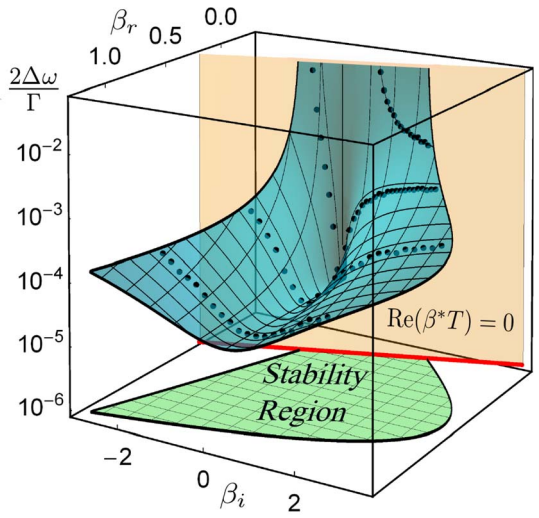

Figure 5 | Dependence of the generation linewidth on the factors β_i and β_r calculated for the relative noise power $\sqrt{p_n/p_s} = 0.015$. The region of stable auto-oscillations is shown by green color (see also Fig. 3a). Analytical result of the equation (10) is shown by the blue surface, numerical results obtained using equation (19) are shown by dots. The region of stable auto-oscillations is shown on the plane below surface. Low-frequency instability boundary is shown by the red line in the plane and by the light yellow plane in space.

Discussion

Figs. 4 and 5 demonstrate that the divergence of the phase-locking bandwidth or the generation linewidth of a non-isochronous auto-oscillator with delayed feedback takes place only near the low-frequency boundary of the auto-oscillation stability region defined by the equation (23), while the behavior of the same quantities near all the other boundaries of the auto-oscillation stability region is regular. Thus, the low-frequency boundary of the stability region has special importance for the non-autonomous behavior of an auto-oscillator.

If in an auto-oscillator we have means to control the magnitude or/and sign of the nonlinear frequency shift β_i (or/and the detuning $\delta\omega_0$ at which the stable auto-oscillation takes place), we could control the phase-locking bandwidth and the generation linewidth of the auto-oscillator.

The situations when the magnitude and even the sign of the nonlinear frequency shift could be controlled by changing a certain external parameter of the auto-oscillator are not rare. In particular, in a spin-torque nano-oscillator it is possible to change the magnitude and the sign of β_i simply by changing the direction or/and the magnitude of the external bias magnetic field (see Fig. 6 in[7]), or by changing the bias direct current driving the device (see Fig. 1d in[33]). Of course, for a normal auto-oscillator with saturation nonlinearity ($\beta_r > 0$) the minimum linewidth is achieved when the auto-oscillator is isochronous, $\beta_i = 0$, which is well-known from the standard auto-oscillator theory[7] (see also Figs. 4 and 5), but if we need to synchronize many auto-oscillators with different oscillation frequencies or switch an individual oscillator from a coherent auto-oscillation regime to a regime of generation of noise-like signals having a wide frequency spectrum, we could use the above described regime of off-resonance generation in a non-isochronous auto-oscillator and bring this device close to the low-frequency boundary of the stability region defined by the condition (23).

In conclusion, we found that in a non-isochronous auto-oscillator with a time-delayed feedback it is possible to achieve an extremely high sensitivity to the external driving signal, and, therefore, to get an unusually large synchronization band near the low-frequency boundary of the auto-oscillations stability region. The understanding of the above described behavior of the auto-oscillator sensitivity could be also fundamentally important for the understanding of synchronization properties in biological systems and for the better understanding of the nature of some diseases, for example – heart arrythmia.

Methods

Analytical calculations. To derive the effective phase equation (7) and expression (8) for the phase sensitivity, we represented the external signal $\xi(t)$ as a continuous sequence of δ-kicks, $\xi(t) = \int\xi(t')\delta(t-t')dt'$, evaluated phase response of the oscillator to a single δ-kick $\xi(t')\delta(t-t')$, and summed up responses from different kicks. The solution of equation (3) under the influence of one *weak* δ-impulse is close to the free-running solution and can be easily found using standard perturbation methods, namely, by linearizing equation (3) near the unperturbed solution (4).

To calculate analytically the synchronization bandwith $\Delta\omega_{PL}$ equation (9), we used the periodic external signal $\xi(t) = Ae^{-i\omega_e t}$ in the phase equation (7) and looked for stationary phase-locked solutions of the form $\phi(t) = -\omega_e t + \Delta\phi$, where $\Delta\phi$ is an arbitrary constant phase shift. The condition for existence of such solutions can be written in the form $|\omega_e - \omega_s| < \Delta\omega_{PL}$, where the phase-locking bandwidth $\Delta\omega_{PL}$ is given by the equation (9).

Similarly, substituting white gaussian noise with known statistical properties for the external signal $\xi(t)$ one can get the generation linewidth $\Delta\omega$ of the auto-oscillator (see Supplementary materials for details).

Numerical methods. To check the above derived analytical results the differential equation describing a nonisochronous auto-oscillator with delay (19) was solved for different forms of the weak external signal $\xi(t)$ using the method of slowly varying amplitudes, where all the frequencies were normalized to the linear damping parameter Γ (or linear relaxation frequency). The equation was solved by a Runge-Kutta method of the 4-th order.

To calculate the phase-locking bandwidth a purely sinusoidal periodic signal of the small amplitude $A/(\Gamma\sqrt{p_s}) = 0.01$ has been added as the right-hand-side part $\xi(t)$ of equation (19). The phase-locking bandwidth has been obtained by varying the fre-

quency of the external signal and determining the frequency of the auto-oscillation for each value of the external driving frequency.

To calculate the generation linewidth external white noise $\xi(t)$ in the right-hand-side part of equation (19) was simulated by random points at regular time intervals with normal distribution of the amplitude. These points were locally interpolated by a 3-rd order polynomial for the continuity of the function. The upper cut-off frequency of the noise was chosen to be 4 times larger than the relaxation frequency (Γ) in equation (19), which is the largest characteristic frequency of the model. The correlation function for the phase of auto-oscillations was determined after solving (19) numerically, and the generation linewidth was obtained from this correlation function.

To find the region of parameters where auto-oscillations are stable we analyzed the possibility of decay of stationary auto-oscillations with the frequency ω_s into oscillations with the frequencies $\omega_s \pm \Omega$ under the action of small perturbations. As it follows from the Lyapunov criteria the auto-oscillations are stable when $\mathrm{Im}(\Omega) < 0$ (see Supplementary materials).

1. Rubiola, E. *Phase Noise and Frequency Stability in Oscillators* (Cambridge University Press, New York, 2009).
2. Glass, L. Synchronization and rhythmic processes in physiology. *Nature* **410**, 277–284 (2001).
3. Epstein, I. R. & Pojman, J. A. *An Introduction to Nonlinear Chemical Dynamics* (Oxford University Press, New York, 1998).
4. Puu, T. *Attractors, Bifurcations and Chaos: Nonlinear Phenomena in Economics* (Springer-Verlag Berlin Heidelberg, 2003).
5. Pykovsky, A., Rosenblum, M. & Kurths, J. *Synchronization: A Universal Concept in Nonlinear Science* (Cambridge University Press, New York, 2003).
6. Chernikov, A. & Schmidt, G. Conditions for synchronization in Josephson-junction arrays. *Phys. Rev. E* **52**, 34153419 (1995).
7. Slavin, A. N. & Tiberkevich, V. S. Nonlinear auto-oscillator theory of microwave generation by spin-polarized current. *IEEE Transaction on Magnetics* **45**(4), 1875–1910 (2009).
8. Ruotolo, A. *et al*. Phase-locking of magnetic vortices mediated by antivortices. *Nature Nanotechnology* **4**, 528–532 (2009).
9. Grollier, J., Cros, V. & Fert, A. Synchronization of spin-transfer oscillators driven by stimulated microwave currents. *Phys. Rev. B* **73**, 060409(R) (2006).
10. Tiberkevich, V. S., Slavin, A. N., Bankowski, E. & Gerhart, G. Phase-locking and frustration in an array of nonlinear spin-torque nano-oscillators. *Appl. Phys. Lett.* **95**, 262505 (2009).
11. Leeson, D. B. A simple model of feedback oscillator noise spectrum. *Proc. IEEE* **54**(2), 329 (1966).
12. Razavi, B. Analysis, modeling and simulation of phase noise in monothilic voltage-controlled oscillators. Paper presented at Custom Integrated Circuits Conference, Santa Clara, CA, USA, DOI:10.1109/CICC.1995.518195 (1995, May).
13. Robins, W. P. *Phase Noise in Signal Sources* (U.K. Peter, Stevenage, 1991).
14. Lee, T. H. & Hajimiri, A. Oscillator phase noise: a tutorial. *IEEE J. Solid-State Circuits* **35**(3), 326–336 (2000).
15. Hajimiri, A. & Lee, T. H. A general theory of phase noise in electrical oscillators. *IEEE J. Solid-State Circuits* **33**(2), 179 (1998).
16. Demir, A., Mehrotra, A. & Roychowdhury, J. Phase noise in oscillators: a unifying theory and numerical methods for characterization. *IEEE Transactions on Circuits and Systems: Fundamental Theory and Applications* **47**(5), 655–674 (2000).
17. Keller, M. W., Pufall, M. R., Rippard, W. H. & Silva, T. J. Nonwhite frequency noise in spin torque oscillators and its effect on spectral linewidth. *Phys. Rev. B* **82**, 054416 (2010).
18. Kaka, S. *et al*. Mutual phase-locking of microwave spin torque nano-oscillators. *Nature* **437**, 389–392 (2005).
19. Hoppensteadt, F. C. & Izhikevich, E. M. Synchronization of laser oscillators, associative memory, and optical neurocomputing. *Phys. Rev. E* **62**(3), 4010 (2000).
20. Rezavi, B. A study of injection locking and pulling in oscillators. *IEEE J. Solid-State Circuits* **39**, 1415–1424 (2004).
21. Strogatz, S. H. *Sync: The Emerging Science of Spontaneous Order* (Hyperion Press, New York, 2003).
22. Ringwood, J. V. & Malpas, S. C. Slow oscillations in blood pressure via a nonlinear feedback model. *AJP Regulatory Integrative and Comparative Physiology* **280**(4), R1105–R1115 (2001).
23. Scholl, E., Hiller, G., Hovel, P. & Dahlem, M. Time-delayed feedback in neurosystems. *Phil. Trans. R. Soc. A* **367**(1891), 1079–1096 (2009).
24. Popovych, O. V., Hauptmann, C. & Tass, P. A. Control of neuronal synchrony by nonlinear delayed feedback. *Biological Cybernetics* **95**(1), 69–85 (2006).
25. Ekeberg, O. A combined neuronal and mechanical model of fish swimming. *Biological Cybernetics* **69**(5–6), 363–374 (1993).
26. Willner, B. E. & Miranker, W. L.Chien-Ping Lu Neural organization of the locomotive oscillator. *Biological Cybernetics* **68**(4), 307–320 (1993).
27. Wang, Hu *Dynamics of Controlled Mechanical Systems with Delayed Feedback* (Springer-Verlag Berlin Heidelberg, 2002).
28. Schultheiss, N., Prinz, A. & Butera, R. (Eds.) Phase Response Curves in Neuroscience: Theory, Experiment, and Analysis. *Springer Series in Computational Neuroscience* **6** (2012).
29. Schuster, H. G. & Wagner, P. Mutual entrainment of two limit cycle oscillators with time delayed coupling. *Prog. Theor. Phys.* **81**, 939–945 (1989).
30. Yeung, M. K. S. & Strogatz, S. H. Time delay in the Kuramoto model of coupled oscillators. *Phys. Rev. Lett.* **82**, 648–651 (1999).
31. D'Huys, O., Vicente, R., Erneux, T., Danckaert, J. & Fischer, I. Synchronization properties of network motifs: Influence of coupling delay and symmetry. *Chaos* **18**, 037116 (2008).
32. Popovych, O. V., Krachkovskyi, V. & Tass, P. A. Phase-locking swallows in coupled oscillators with delayed feedback. *Phys. Rev. E* **82**, 046203 (2010).
33. Urazhdin, S., Tiberkevich, V. & Slavin, A. Parametric excitation of a magnetic nanocontact by a microwave field. *Phys. Rev. Lett.* **105**, 237204 (2010).

Acknowledgments

This work is supported by DARPA MTO/MESO grant N66001-11-1-4114, by the U.S. Army Contract from TARDEC, RDECOM, and by the grant DMR-1015175 from the National Science Foundation of the USA.

Author contributions

The statement of the problem belongs to A.N.S. and H.X.T. V.S.T. proposed the general framework and theoretical approach of the problem and made calculations of stability diagram. R.S.K. developed analytical results and numerical calculations of the generation linewidth and phase-locking bandwith. All authors analyzed the data and participated in the preparation of the manuscript. A.N.S. and H.X.T. supervised the project.

Additional information

Supplementary information accompanies this paper at http://www.nature.com/scientificreports

Competing financial interests: The authors declare no competing financial interests.

How to cite this article: Tiberkevich, V.S., Khymyn, R.S., Tang, H.X. & Slavin, A.N. Sensitivity to external signals and synchronization properties of a non-isochronous auto-oscillator with delayed feedback. *Sci. Rep.* **4**, 3873; DOI:10.1038/srep03873 (2014).

This work is licensed under a Creative Commons Attribution-NonCommercial-ShareAlike 3.0 Unported license. To view a copy of this license, visit http://creativecommons.org/licenses/by-nc-sa/3.0